

Low-frequency earthquakes at the Torfajökull volcano, south Iceland

Heidi Soosalu ^{a,*}, Regina Lippitsch ^b, Páll Einarsson ^{c,1}

^a *Nordic Volcanological Center, University of Iceland, Sturlugata 7, 101 Reykjavik, Iceland*

^b *Bullard Laboratories, Department of Earth Sciences, University of Cambridge, Madingley Road, Cambridge, CB3 0EZ, UK*

^c *Institute of Earth Sciences, University of Iceland, Sturlugata 7, 101 Reykjavik, Iceland*

Received 7 March 2005; received in revised form 1 June 2005; accepted 31 October 2005

Available online 30 January 2006

Abstract

Torfajökull is a large rhyolitic volcanic edifice with a 12-km-diameter caldera and abundant high-temperature geothermal activity. It is located in the neovolcanic zone in south Iceland, at the junction of the eastern rift zone and a transform zone with the intraplate volcanic flank zone of south Iceland. The latest eruption at Torfajökull occurred about 500 years ago. Torfajökull is a source of persistent small-scale seismicity, where two types of earthquakes occur. High-frequency events are concentrated in the western part of the caldera and low-frequency events cluster in the south. Small low-frequency earthquakes have been observed at Torfajökull since the installation of a local analogue seismograph station in 1985. They typically occur in swarms; up to 300 earthquakes per day have been observed. The low-frequency events have a frequency content of about 1–3 Hz, and are difficult to locate, because of the emergent nature of their phases. The 160 events located during the years 1994–2000 using the permanent Icelandic seismic network cluster in the southern part of the Torfajökull caldera. A closer study of low-frequency events was carried out between May and October 2002, with a dense network of twenty Güralp 6TD broadband seismometers in the Torfajökull area. No distinct swarm activity was observed during this period, but small low-frequency events occurred almost on a daily basis. About 330 low-frequency events were detected during the study period. They are located in the southern part of the caldera, between two small glaciers. Areas of intensive geothermal activity surround the cluster of low-frequency events. It is argued that these earthquakes are associated with active magma in the south part of the Torfajökull caldera, possibly a rising cryptodome. © 2005 Elsevier B.V. All rights reserved.

Keywords: Torfajökull volcano; Iceland; low-frequency earthquakes; cryptodome

1. Introduction

Iceland is a unique landmass situated astride the Mid-Atlantic ridge. Its geology is characterised by the interplay between spreading at the mid-oceanic plate

boundary and a hot spot, which has a centre located in east-central Iceland (Wolfe et al., 1997). The North American and Eurasian plate drift apart with a velocity of approximately 2 cm/year. The plate boundary in Iceland is located within the neovolcanic zone, a chain of active volcanoes, which traverses the central part of Iceland (Fig. 1). In the south it has two branches, the Western and the Eastern volcanic zone, connected by a transform, the South Iceland seismic zone. In the north there is a single Northern volcanic zone. North of Iceland the plate boundary is displaced to the west by the Tjörnes fracture zone (Fig. 1).

* Corresponding author. Present address: Bullard Laboratories, Department of Earth Sciences, University of Cambridge, Madingley Road, Cambridge, CB3 0EZ, UK. Tel.: +44 1223 337 188; fax: +44 1223 360 779.

E-mail addresses: heidi@hi.is (H. Soosalu), palli@hi.is (P. Einarsson).

¹ Tel.: +354 525 4816; fax: +354 552 1347.

Volcanism within the neovolcanic zone is expressed by volcanic systems, which consist of a central volcano—the location of highest productivity—and a fissure swarm transecting it (e.g. Jakobsson, 1979; Björnsson and Einarsson, 1990). The central volcano Torfajökull (Figs 1 and 2), the largest rhyolitic complex in Iceland 450 km² in area, rises about 500 m above the surrounding basaltic landscape (Gunnarsson et al., 1998). Its WNW–ESE axis is 30 km long, while its NNE–SSW axis is 18 km long (McGarvie, 1984), and its caldera is 12 km in diameter (Sæmundsson, 1972, 1982). Torfajökull has fissure swarms stretching to the NE and SW of the central volcano. North of Torfajökull the volcanic zone is characterised by rifting activity and to the south it has the nature of a non-rifting flank zone. At the site of Torfajökull rifting is propagating towards southwest (Óskarsson et al., 1982).

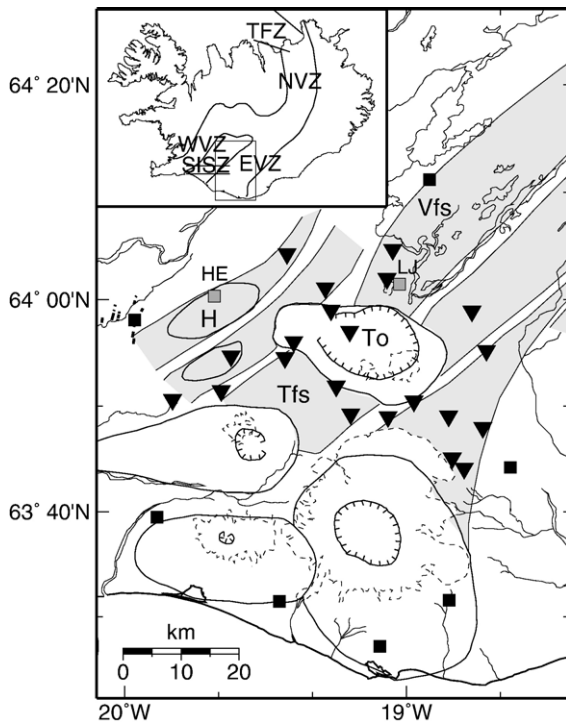


Fig. 1. Index map of the Torfajökull area. Black inverted triangles are seismic stations of the 2002 temporary network. Black squares are digital SIL stations and grey squares the analogue stations LJ and HE. The central volcanoes are outlined, their fissure swarms are shaded grey (Einarsson and Sæmundsson, 1987) and the calderas are hatched (Jóhannesson et al., 1990). Thick black lines approximately at 64°N and 20°W are faults of the South Iceland seismic zone. To stands for Torfajökull, Vfs for Veidivötn fissure swarm, Tfs for Torfajökull fissure swarm and H for Hekla. Dashed lines mark the glaciers and thin solid lines outline rivers and lakes. The smaller index map shows the locations of the areas related to the plate margin: Western (WVZ), Eastern (EVZ) and Northern (NVZ) volcanic zones, South Iceland seismic zone (SISZ) and Tjörnes fracture zone (TFZ).

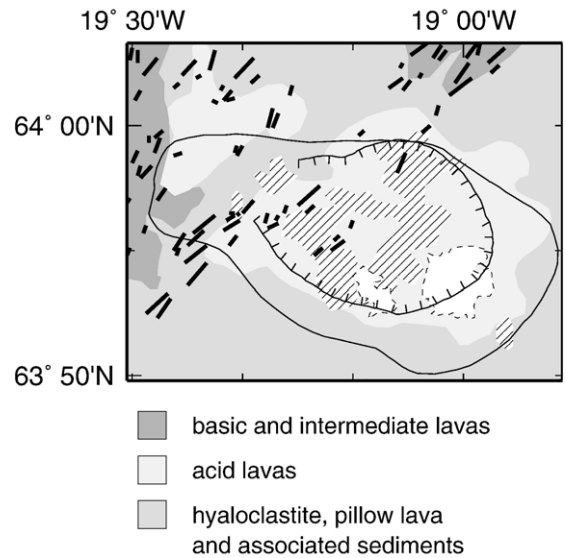


Fig. 2. General outlines of the geology of the Torfajökull region (Jóhannesson and Sæmundsson, 1989). Approximate locations of the geothermal fields are rastered and black bars sketch postglacial eruption sites (from Jóhannesson et al., 1990).

Being a major centre of almost exclusively acidic volcanism, Torfajökull is geologically anomalous in the context of the spreading plate boundary. The eruption products of Torfajökull itself are rhyolitic, but two kinds of basaltic magma have been mixed with it. One of the basalts is laterally injected tholeiite from the ~100-km-long Veidivötn fissure swarm northeast of Torfajökull (Fig. 1). The other is olivine basalt from its own magma system (Larsen, 1984; McGarvie, 1984). The latest eruption in the Torfajökull area occurred at the end of the fifteenth century (Larsen, 1984). Ash zone Z-2 in Atlantic sediments and Greenland ice cores is thought to have originated from a major eruption of Torfajökull about 52,000 years ago (Grönvold et al., 1995).

The Torfajökull central volcano contains one of the most powerful high-temperature geothermal fields in Iceland (Arnórsson et al., 1987) (Fig. 2). The activity is grouped into geothermal areas, many of which are within or around the area of recent postglacial rhyolite eruptions. Individual geothermal features are scattered throughout the entire complex but are much less common in the eastern part (McGarvie, 1985).

Seismically Torfajökull is characterised by persistent small-scale activity. Two sorts of events are observed, and they do not overlap spatially or temporally (Soosalu and Einarsson, 1997). High-frequency earthquakes, with local magnitudes typically smaller than M_L 3 occur frequently in the western part of Torfajökull (Einarsson, 1991; Soosalu and Einarsson, 1997; Lip-

pitsch et al., 2005). After the installation of an analogue vertical-component seismometer in the area in 1985, low-frequency Torfajökull earthquakes were discovered (Brandsdóttir and Einarsson, 1992). Their magnitudes are generally smaller than M_L 1 and they often occur in swarms. Tentative locations made by Soosalu and Einarsson (2004) suggest an origin in the southern part of the Torfajökull caldera.

A network of twenty portable three-component seismometers was installed in the Torfajökull area in the summer of 2002 in order to observe the seismicity, especially low-frequency events, in more detail. Additional data are provided by the digital Icelandic national SIL (South Iceland Lowland) network and two local, vertical-component analogue stations. Our purpose is to describe and interpret the nature and temporal behaviour of the low-frequency events, locate their origin and seek explanations for their causes. Concluding from our observations and geological character of Torfajökull we

suggest that the low-frequency seismicity is linked to the existence of a cryptodome, a dome-shaped structure created by the ascent of viscous magma and its accumulation at shallow depth.

2. The seismic network and data set

Torfajökull low-frequency events have been observed since the deployment of the local analogue station LJ (see Fig. 1), north of the Torfajökull caldera in 1985 (Brandsdóttir and Einarsson, 1992). The analogue seismograms of the station LJ and a second station HE, on the flank of the Hekla volcano approximately 30 km away, provide a qualitative estimate on the occurrence of Torfajökull low-frequency events throughout the last two decades.

In 1990 the SIL network of eight three-component digital seismometers was installed in south Iceland (Stefánsson et al., 1993). The network, later expanded

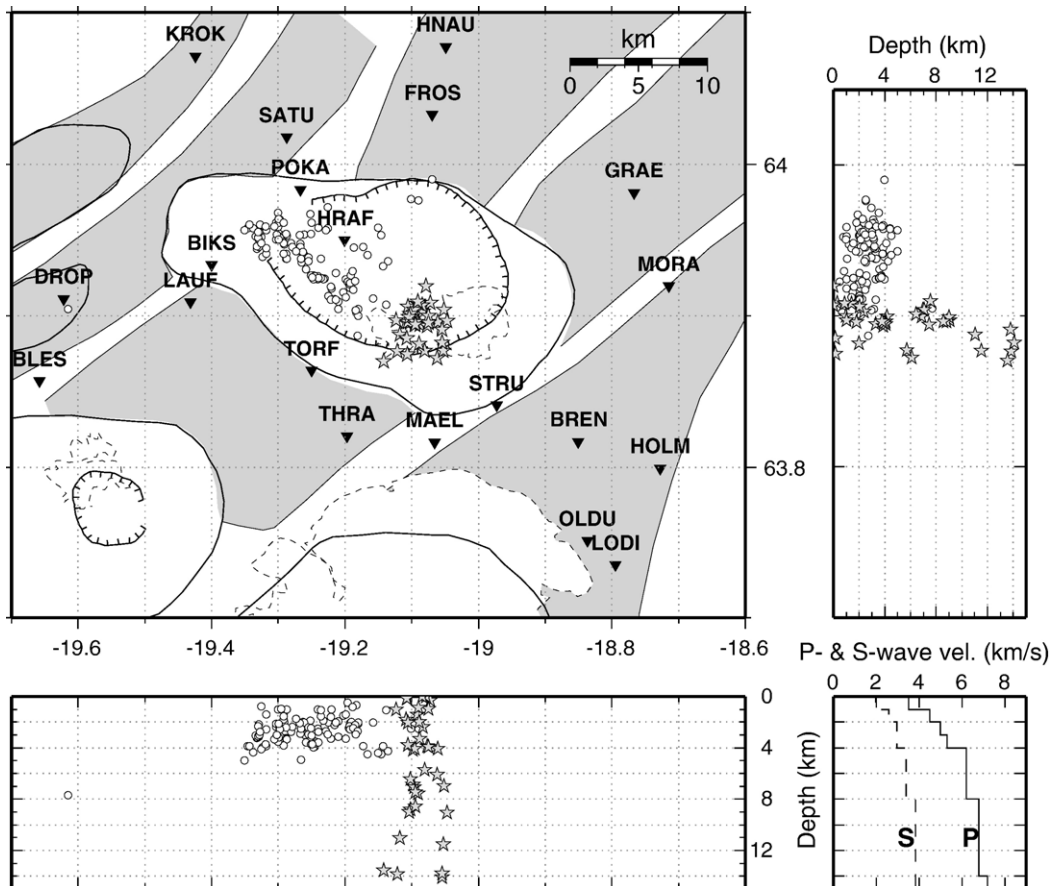


Fig. 3. Temporary seismic network (black inverted triangles) and recorded seismicity at Torfajökull in 2002. Earthquake locations are shown in map view, and E–W and N–S vertical sections. Open circles are high-frequency events as described in Lippitsch et al. (2005). Grey stars denote the 38 low-frequency events with best locations, located with the program NonLinLoc. Velocity model used for relocation is shown in lower right corner.

to other parts of the country (Böðvarsson et al., 1999), is maintained by the Icelandic Meteorological Office. With these stations the largest low-frequency events can be detected. However, location accuracy is poor, because station-event distances are 25 km or more, and emergent onsets of the low-frequency events impair the reading precision.

Between May and October 2002 a network of twenty broadband Guralp 6TD three-component seismometers was deployed in the Torfajökull area to study low-frequency earthquakes in more detail (Figs. 1 and 3). The sampling rate was set to 50 samples/s, and the instruments measured continuously. Earlier studies (Soosalu and Einarsson, 2004) indicated that low-frequency earthquakes cluster in the southern part of the caldera. Hence, the network was designed to record these low-frequency events and to be logistically functional. The latter point is a challenge in remote areas like the Torfajökull region with its rough terrain. Sites must be relatively easy to reach to ensure effective station maintenance. Thus, all stations were mounted next to mountain tracks, leaving the poorly accessible eastern part of the caldera without stations.

Low-frequency events have small amplitudes and emergent onsets of phases. Event detection is, therefore, not straightforward and has to be done manually. Seismograms of the two or three closest stations (HRAF, MAEL, STRU, THRA, TORF, depending on availability) were examined for the entire study period, and low-frequency events were visually identified. About 330 low-frequency events were detected in total. To locate these events, we initially used the location program HYPOINVERSE (Klein, 1978), with a crustal model consisting of layers with constant velocity gradient (Soosalu and Einarsson, 1997). The 38 best events (root mean square travel time residual (rms) ≤ 0.18 s, horizontal standard error (erh) ≤ 0.9 km, vertical standard error (erz) ≤ 1.6 km, largest gap between observing stations 46–143°, and 5–13 P-readings) were used in further, refined analysis.

Lippitsch et al. (2005) analysed the high-frequency events observed in the Torfajökull region. They calculated a 1D velocity model (Fig. 3) for the region by jointly inverting for hypocentre and origin time. To obtain more reliable hypocentre locations and better estimates on the location error, we used the non-linear location program NonLinLoc (Lomax et al., 2000; Lomax and Curtis, 2001) in combination with this velocity model. The resulting event locations give an improved image of the low-frequency activity and are used as the basis for our interpretation.

3. Features of seismic activity in the Torfajökull area

Persistent small-scale seismic activity is characteristic for the Torfajökull central volcano. Two event populations are observed: high-frequency earthquakes in the western part of the caldera and low-frequency earthquakes in the south (Fig. 3). The clusters of these two types of events do not overlap either spatially or temporally (Soosalu and Einarsson, 1997). Fig. 4 shows example seismograms for both types of earthquakes recorded at station HRAF, located inside the caldera. High-frequency events have a typical frequency range of 4–10 Hz, whereas low-frequency events reveal a narrow frequency band with a peak at ~ 1 –2 Hz.

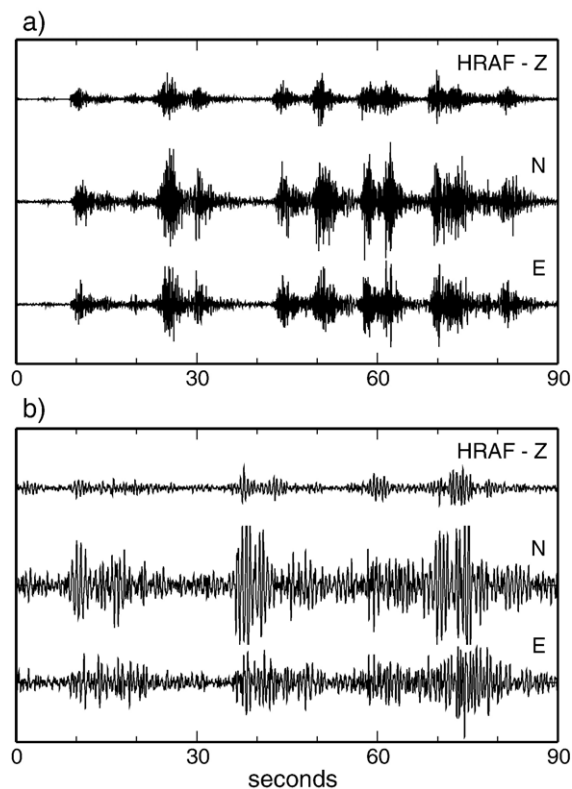


Fig. 4. Example waveforms (components: Z—vertical, N—north and E—east) of swarms of both types of Torfajökull earthquakes recorded by station HRAF. a) High-frequency events, in <5 km distance from HRAF. The data are high-pass filtered at 0.8 Hz for excluding microseismic noise. The channels are in same arbitrary scale and the N component is clipped because of illustrating purposes. b) Low-frequency events, in ~ 7 km distance from HRAF. The data are band-pass filtered at 0.8–6.0 Hz. The three channels are in same arbitrary scale, the N component is clipped because of illustrating purposes.

3.1. High-frequency earthquakes

Small (M_L typically <3) high-frequency earthquakes are a well-known, permanent feature in the western part of the Torfajökull caldera and further to the west (Einarsson, 1991; Soosalu and Einarsson, 1997). Such events are mainly restricted to the geothermal fields within the volcanic region and do not occur in the southern or eastern part of the caldera. Because of their distribution and the persistence of seismicity in Torfajökull, Einarsson (1991) suggested that heat mining and thermal cracking cause these high-frequency events.

Soosalu and Einarsson (1997) analysed high-frequency earthquakes at Torfajökull, which occurred between 1990 and 1995. The data set consisted of approximately 160 events, about 80 of which were “well-located” (with the criteria: $rms \leq 0.2$ s, $erh \leq 1.0$ km, $erz \leq 2.0$ km, and $gap \leq 180^\circ$). Their event locations show a spherical distribution of hypocentres in the uppermost 13 km. Within this cluster an aseismic volume was found, with a radius of about 4 km and a centre at about 8 km depth. This feature was interpreted as a cooling magma chamber, not molten but in a ductile state (Soosalu and Einarsson, 1997, 2004). The high-frequency earthquakes were interpreted as the result of thermal cracking around the cooling body, assisted by deep circulation of geothermal water.

Lippitsch et al. (2005) studied the high-frequency earthquakes that were detected by the portable network which operated during the summer of 2002, and nine surrounding SIL stations. With the aim to obtain precise hypocentral relocations they constructed an improved 1-dimensional velocity model, used the non-linear location program NonLinLoc (Lomax and Curtis, 2001), and further calculated relative locations of correlated event pairs using the program HypoDD (Waldhauser and Ellsworth, 2000, 2002). They relocated 121 of these events, with local magnitudes of 0.2 to 2.3. These events cluster tightly at shallow depths (0–6 km). The study confirmed that Torfajökull high-frequency earthquakes occur only in the western part of the caldera.

3.2. Low-frequency earthquakes

Low-frequency events are a persistent feature of Torfajökull seismicity. However, the level of activity varies considerably. They typically occur in swarms, separated by quieter intervals. Fig. 5 shows a statistical view of the number of observed low-frequency events in the years 1991–1995 and 1997–2002, constructed using paper records from the analogue stations LJ and HE, and events detected by the permanent SIL network.

Swarms of low-frequency events begin abruptly, rise quickly to the level of up to a few hundred events per day,

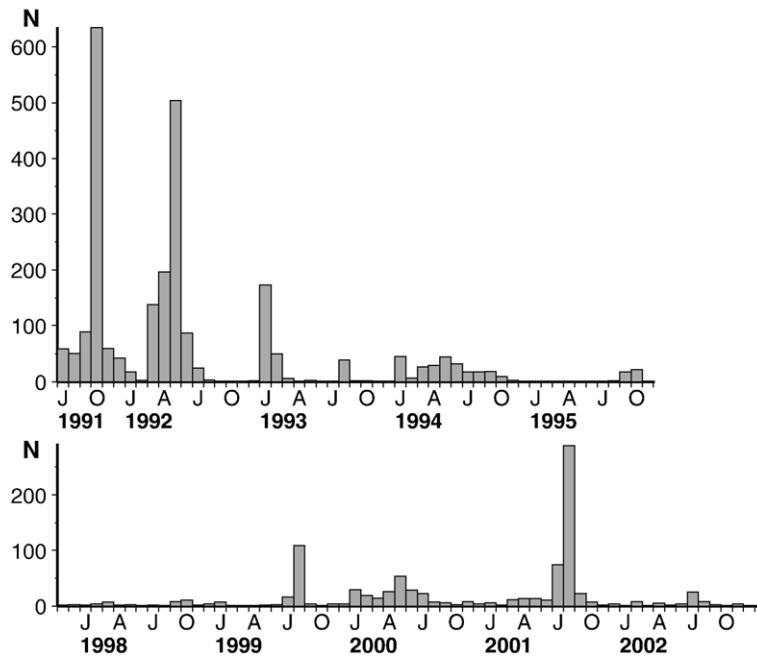


Fig. 5. Histogram showing monthly number of Torfajökull low-frequency events between July 1991 and December 2002, recorded by analogue stations LJ and HE and the SIL network. There is a data gap between December 1995 and October 1997, and observations of the Torfajökull 2002 net are not included.

and can last a few days (Brandsdóttir and Einarsson, 1992; Soosalu and Einarsson, 1997). This sort of swarm activity was distinct after the eruption of the neighbouring volcano Hekla in January–March 1991, in late 1991 and early 1992, with a peak of over 600 events on October 29–31, 1991. Based on earlier observations of Icelandic volcanoes displaying concerted activity, Soosalu and Einarsson (1997) speculated that there is a link between these two volcanoes. However, after the Hekla eruption in February–March 2000 no similar increase in Torfajökull low-frequency event activity was observed.

The permanent seismic stations are capable of detecting the largest of the low-frequency Torfajökull earthquakes. However, locations are poorly constrained, due to the emergent nature and small size of the events, and distance to the closest SIL stations (>25 km). A dense network of seismometers was available for the first time in summer 2002. Although the level of low-frequency seismicity was modest (see Fig. 5), small low-frequency events were detected almost on a daily basis, occasionally occurring in swarms of a few events (Fig. 4b). Sometimes events were merged with each other, resembling tremor. No such burst observed lasted longer than a minute.

Low-frequency earthquakes at Torfajökull are typically small in size, up to M_L 1 and they have similar waveforms. Their P-wave arrivals are very small and emergent, and, hence, hard to identify. Example seismograms of one of the largest events are shown in Fig. 6. There is a later clearer arrival (marked with X), with a considerably larger amplitude than P. These later arrivals are more impulsive than those of P and easier to identify. The radial component has typically the highest amplitudes. Later reverberations are usual, sometimes with strikingly regular waveform and harmonic appearance. The events exhibit a narrow band of frequencies, having a peaked spectrum in the frequency band of 1–3 Hz, mainly within 1–2 Hz (Fig. 7), with little variation in spectrum between the observing stations. The most distinct local feature is that waveforms recorded at station TORF often have a broader spectrum, up to 4–5 Hz.

In the location procedure of low-frequency events we treated phase X as an S-wave arrival. We have conducted tests to check if this assumption is valid. First, we plotted a Wadati diagram with observations of both high- and low-frequency earthquakes, recorded by the temporary network, augmented with earlier low-frequency earthquake data of Soosalu and Einarsson (2004) (Fig. 8). The linear regression indicates a V_p/V_s ratio of 1.77, high- and low-frequency events following

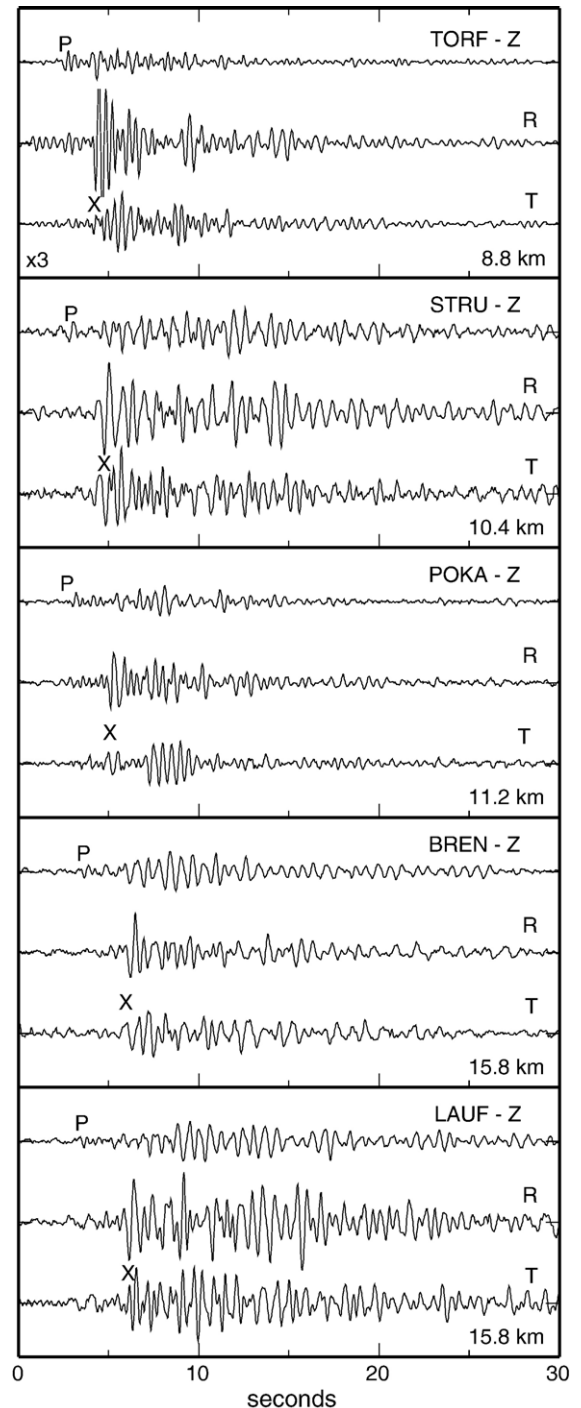


Fig. 6. Velocity seismograms of a low-frequency event on July 29, 2002, $63^{\circ} 54.25'N$, $19^{\circ} 05.81'W$, at 7 km depth, with M_L 0.7. Components are rotated: Z—vertical, R—radial, T—transverse and the data band-pass filtered at 0.8–8.0 Hz. Distance to stations is shown in the low right. The seismograms of TORF (R-component clipped for presentation purposes) are three times larger than all the others, which are in the same arbitrary scale. P-arrivals and a later phase (X) are marked.

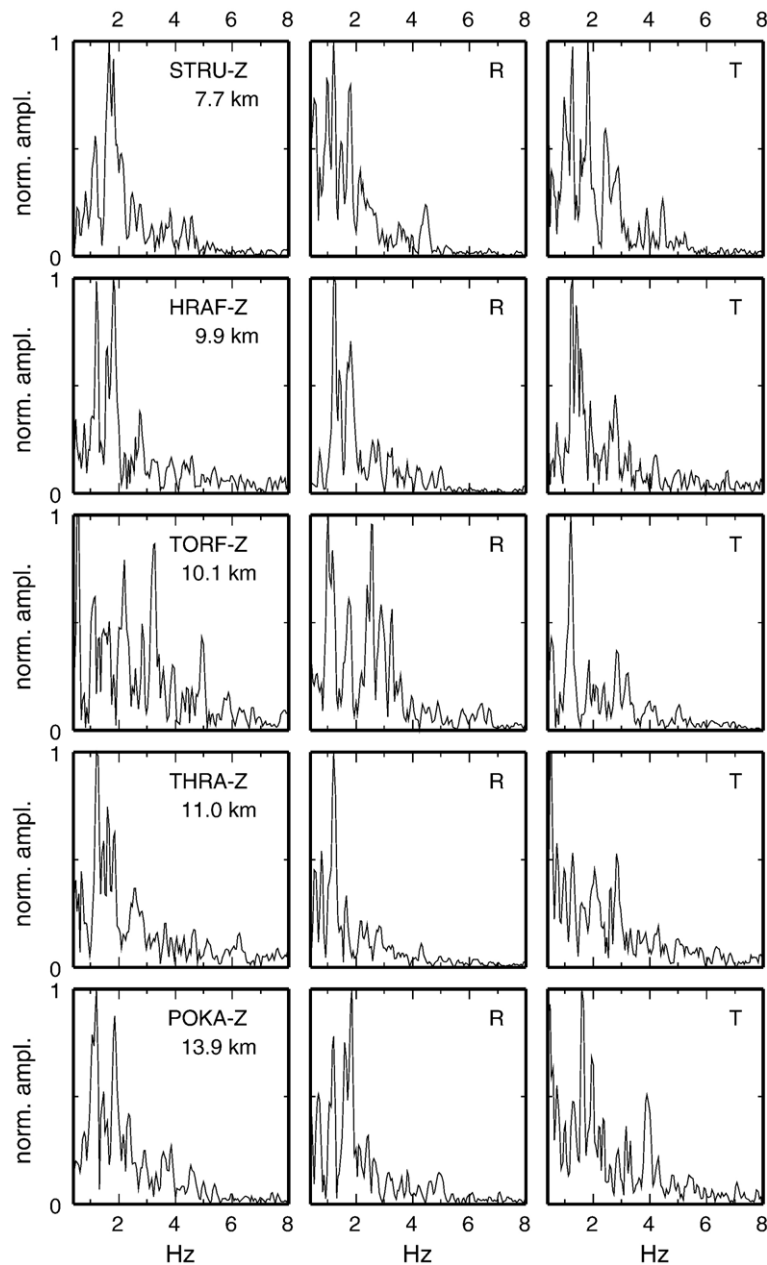


Fig. 7. Examples of spectra of a low-frequency event, July 19, 2002, M_L 0.8. Distance to the event is shown for each station. Z—vertical, R—radial, T—transverse component. The spectra are clipped at 0.4–8.0 Hz, as below 0.4 Hz microseismic noise is dominant and above 8.0 Hz peaks are of negligible size.

the same line. This indicates that phase X is indeed an S-wave arrival.

In a second test we examined the validity of assumption of phase X being an S by relocating the events with (i) P-readings only and (ii) with P and X, assuming phase X=S. We performed several relocation runs with the depth fixed, using the location program Hypoellipse (Lahr, 1999) and the 1-dimensional crustal model of

Lippitsch et al. (2005). We used the event shown in Fig. 6 (observed by fifteen stations) and fixed its depth at 1 km intervals between 0 and 15 km. The best depth estimate is that for which the root mean square travel time residual (rms) reaches its minimum. We observed small rms (<0.18 s) for depths between 0 and 7 km, with a drastic increase in rms for deeper event locations. The rms value was very similar for depths between 3 and 7 km

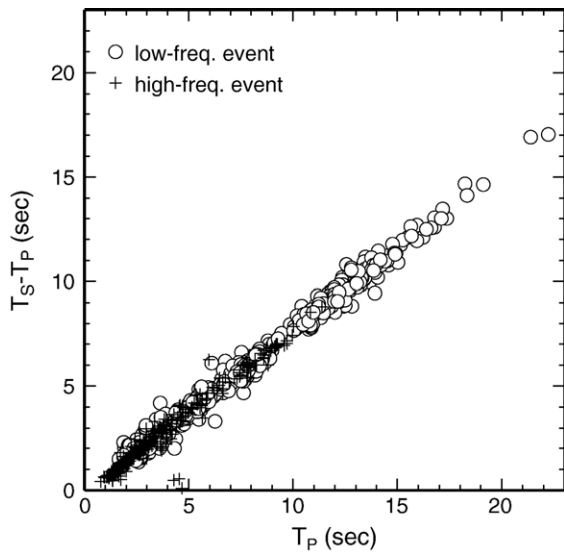


Fig. 8. A Wadati diagram for high- and low-frequency Torfajökull earthquakes. Low-frequency earthquake observations are from Soosalu and Einarsson (2004) and this study, high-frequency events from Lippitsch et al. (2005).

(~ 0.16 s) and had a minimum at 5 km. The non-unique result was to be expected; as the closest stations are about 7 km away, the depth resolution of shallow events is generally not very good. Additionally, the reading error in emergent P-phases increases the location error. However, adding phase X (=S) to the location procedure altered neither the rms nor the hypocentral locations. Differences in the epicentral co-ordinates and rms between the two runs (i) and (ii) were negligible. In comparison, hypocentral depth of 7 km was found with the program NonLinLoc of Lomax and Curtis (2001).

In a third test we plotted particle motion for the same event. The resulting plots are shown in Fig. 9. It illustrates that after the arrival of the phase X there is considerable linear movement in the radial plane, similar to a particle motion expected for a radially polarised S-wave. From these tests we conclude that if phase X is not a direct S-wave, it at least has a similar velocity and particle motion.

3.3. Relocation of low-frequency events

About 330 small low-frequency events were recorded with the temporary Torfajökull network between May and October 2002. For 240 events we could obtain a stable solution for the location using the linear location procedure HYPOINVERSE (Klein, 1978). The resulting epicentres form a diffuse cloud in the southern part of the volcano. We selected 38 high-quality events and made an attempt to improve their hypocentral

locations by calculating a probabilistic, non-linear solution to the location problem with the program NonLinLoc (Lomax et al., 2000; Lomax and Curtis, 2001) using the 1D velocity model calculated by Lippitsch et al. (2005). Two major advantages of this relocation routine are (1) NonLinLoc is a non-linear approach and (2) it provides comprehensive uncertainty and resolution information, represented by a posterior probability density function (PDF) of model parameters. The location algorithms follow the probabilistic formulation of inversion of Tarantola and Valette (1982). In brief, the complete, probabilistic solution can be expressed as a posterior PDF if the calculated and the observed arrival times are assumed to have Gaussian uncertainties expressed by covariance matrices, and if the prior information on origin time is taken as uniform. This assumption allows a direct, analytical evaluation of the PDF for the spatial location and the origin time. A complete description of this formulation is given by Tarantola and Valette (1982) and Moser et al. (1992).

We relocated the 38 events using the Oct-Tree algorithm (Lomax and Curtis, 2001), which uses recursive subdivision and sampling of cells in 3D to generate a cascade of sampled cells. The number of sampled cells follows the values of the PDF at the cell centre, thus leading to a higher density of cells in areas of higher PDF (lower misfit). The solution is fully non-linear and reflects location uncertainties due to the geometry of the network, picking errors of the observed arrival times and travel time calculation errors. The location uncertainties are shown by density scatter plots and the final hypocentral location is given by its maximum likelihood (or minimum misfit) value or by the expectation hypocentral location (Gaussian estimator).

Fig. 10 images the resulting locations (maximum likelihood location) and the corresponding uncertainties visualised by 68% confidence ellipsoids. The map view shows that all 38 events are densely clustered between the three stations HRAF, TORF, and STRU. The confidence ellipsoids indicate an epicentral location error of less than ± 1 km for most cases. The depth plots show that the error in depth is markedly bigger than the horizontal, indicated through vertically elongated ellipses, reaching absolute values of about 5 km.

The location errors are relatively large compared to those obtained for the high-frequency earthquakes (e.g. 500 m horizontal error, 1500 m vertical error in Lippitsch et al., 2005). Main threshold in locating the low-frequency events, apart from the distance to the closest station of about 5–9 km, was the small number of high-quality P-wave arrival time readings. However, with these improved locations we can restrict the occurrence

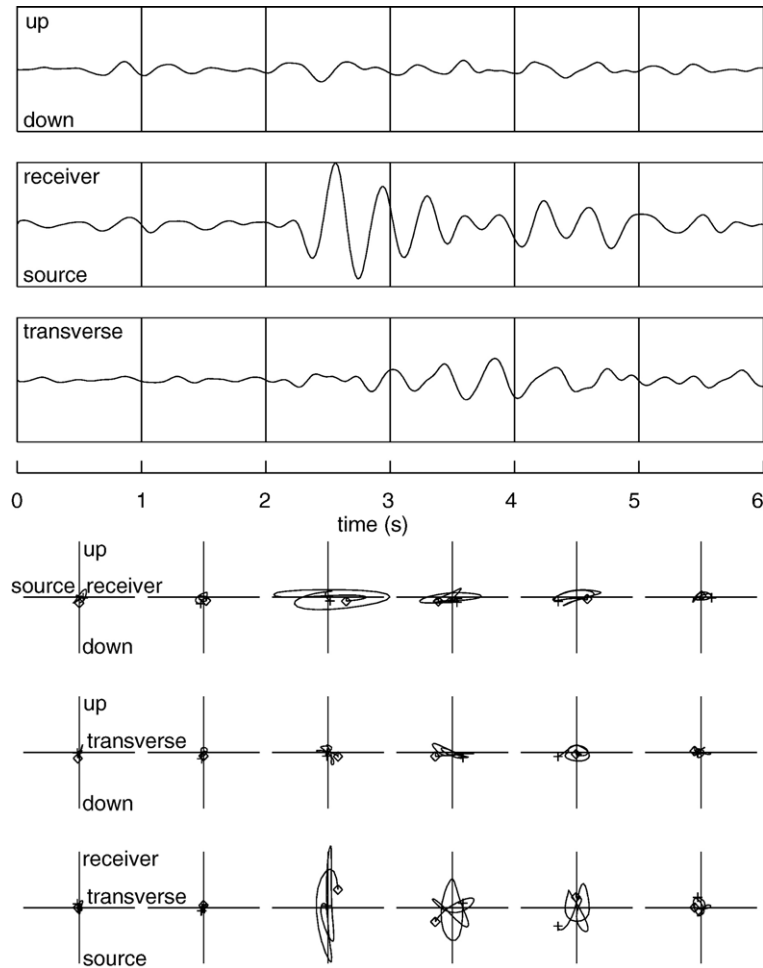


Fig. 9. Velocity seismograms at TORF for the event shown in Fig. 6 with the particle motion plots, second by second starting 0.5 s before the P-onset. A cross marks the start and a diamond the end of motion.

of low-frequency earthquakes to a small area in the southern part of the Torfajökull caldera between the two glaciers. In depth, these events do not exceed 14 km, and are most likely shallower.

Only one of these events (M_L 0.7) was detected by the SIL network. With this magnitude as a reference, we calculated the local magnitudes for the 13 best constrained events with the program Seismic Handler (Stammler, 1992) using the formula

$$M_L = \log_{10}(A) + \sigma$$

where A is the maximum digital amplitude and σ is a tabulated function of epicentral distance in kilometres. For the Torfajökull low-frequency events magnitude values ranged from 0.3 to 0.9, with most of the events near the top of the range.

By calculating the cross-correlation coefficient for S waveforms of the 38 events, we investigated similarities

in these low-frequency events. Two waveforms were considered similar within a tapered 3-s (150 samples) window if the S-wave arrivals had a cross-correlation coefficient greater than 0.75. Most of the events correlated rather well with each other. Fig. 11 shows waveforms from 5 different events recorded at station STRU. The good correlation of these waveforms (Table 1) suggests that the corresponding events occur at the same or a very close by location, and that these events have similar focal mechanisms.

4. Discussion

Low-frequency earthquakes, or long-period earthquakes, are observed at many active volcanoes. These events are generally small in magnitude and in many cases related to ongoing or impending eruptive activity (Minakami, 1974). They often have a higher-frequency

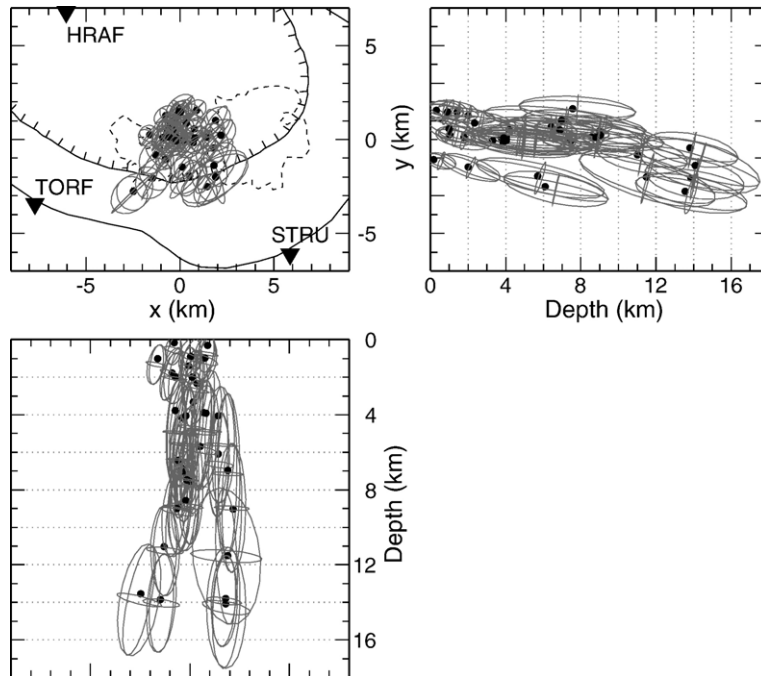


Fig. 10. The best constrained Torfajökull low-frequency events shown with their error ellipsoids, viewed from above, south and east.

onset followed by harmonic waveform containing frequencies between 0.5 and 5 Hz (Chouet, 1996), most typically at 2–3 Hz (McNutt, 2000). P-waves of the low-frequency events are usually emergent and the S-waves are not clear or are absent (Minakami, 1974; McNutt, 2000). Low-frequency events are thought to be caused by fluid pressurization processes such as bubble

formation and collapse, and also by shear failure, tensile failure, or non-linear flow processes which occur at very shallow depths (McNutt, 2000).

The Torfajökull events have many of the general characteristics of low-frequency earthquakes, such as the frequency content (~1–3 Hz), harmonic coda and emergent P-waves. There is, however, a relatively distinct later arrival, which we initially called phase X. Since these events occur within an active volcano, one cannot rely on it being a direct S-wave arrival. Our tests showed that velocity and particle motion of phase X are very similar to those of an S-wave; therefore we used it as an S in our location procedure. High-frequency onsets of the Torfajökull low-frequency events have not been recorded, even at the closest seismic stations 7–8 km away. The occurrence of low-frequency events has not been accompanied by eruptive activity at Torfajökull.

Low-frequency earthquakes similar to those of Torfajökull events have been described at a few other

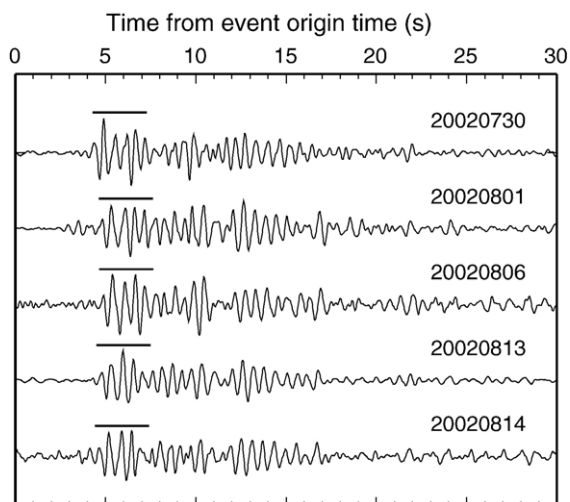


Fig. 11. Example of radial component seismograms for five different events recorded at station STRU. Cross-correlation analysis within a tapered 3-s (150 samples) window, shown with a bar above each seismogram, is performed for these events.

Table 1

Cross-correlation values of S-phases for events shown in Fig. 11

Correlated events	Cross-correlation coefficient
20020730–20020801	0.79
20020730–20020806	0.77
20020730–20020813	0.76
20020730–20020814	0.83

volcanoes. Simiyu and Keller (2000) studied the earthquake activity at the Olkaria geothermal area in the Kenya rift valley. They observed three types of events: monochromatic low-frequency events, higher-frequency events with no clear phases after the onset and events that have characteristics of both of the former groups. Their low-frequency events have a dominant peak at 2 Hz and a smaller peak at 4 Hz. The P- and S-phases of these events are well-defined. Simiyu and Keller remark that these signals are from deep events and are probably related to volcano-tectonic activity.

Sherburn et al. (1999) describe the seismicity at the andesitic volcano Ruapehu in New Zealand. Among other seismic signals, they detected low-frequency volcanic events that have some similarities with those detected at Torfajökull. They have an emergent onset, are typically multiple events and have a sharply peaked spectrum at about 2 Hz. These volcanic events can have far larger magnitudes (up to M_L 4) than have been observed at Torfajökull, and they were observed to accompany phreatic and phreatomagmatic eruptions.

As volcanoes rise above their surroundings, they often are covered by ice caps. At Torfajökull there are two small glaciers at the southern rim of its caldera. In some cases low-frequency events observed at volcanoes are interpreted as being related to glacial processes, not to volcanic activity. For example, Weaver and Malone (1976) studied low-frequency events at Mt. St. Helens with a local network. Due to the shallow depth of the events and restriction to glaciated areas they were interpreted as ice-related. Ruiz et al. (1998) studied low-frequency events at the Cotopaxi volcano in Ecuador and found events with emergent phases like those at Torfajökull, but not occurring in swarms. These events take place at depths between 4 km a.s.l. and 8 km b.s.l., and are believed to be triggered by interaction between magmatic heat and ground water, originating from glacial thaw water. Almendros et al. (1997) draw similar conclusions on the origin of volcanic tremor at Deception Island, Antarctica. They interpret the tremor to consist of superimposed hybrid events, caused by interaction between thaw water and hot materials in a shallow aquifer.

Well-constrained locations of Torfajökull low-frequency events indicate that glacial processes are unlikely to be direct sources of these earthquakes. The activity is clearly centred between the two glaciers, not underneath them. However, the glaciers at Torfajökull contribute to the groundwater system in the southern part of the caldera and can have a secondary effect on the seismicity, similar to the activity at Cotopaxi and Deception Island.

Bjarnason and Ólafsson (2000) studied the chemical composition of steam and water in geothermal springs at several locations within the Torfajökull caldera. They determined temperatures in hot springs from the chemical compounds detected in the samples. For instance, their temperature estimates using CO_2 indicate that the hottest values (≥ 350 °C) are found in springs in the southern part of the caldera. Heavy alteration of minerals observed in these locations supports their interpretation (Bjarnason, J.Ö., pers. comm., 2004). The locations of the low-frequency earthquakes coincide with the geochemically defined hottest areas.

Soosalu and Einarsson (2004) suggested that the low-frequency seismicity at Torfajökull is related to active magma, while high-frequency earthquakes are indications of seismicity linked to hydrothermal cooling of another magma volume. Our current study is in harmony with this view. Torfajökull low-frequency earthquakes are very localised, within a single area of diameter of 5 km, supported by our event locations and the very similar appearance of their waveforms. These observations together with the geochemical observations and the rhyolitic geology lead us to propose that this seismicity is closely related to a cryptodome at the locality where low-frequency earthquakes occur. A cryptodome can be defined as a body of viscous magma which has risen to a high level in the crust. It actively deforms adjacent strata, but does not break through to the surface (Riggs and Carrasco-Nunez, 2004). Current cryptodoming activity has been witnessed at some acidic volcanoes in the world, such as Mt. St. Helens in the U.S. (e.g. Donnadieu et al., 2001) and Usu in Japan (Okada et al., 1981). In Iceland, a similar cryptodome interpretation has been suggested for the clustered seismicity at the Goðabunga rise within Katla volcano south of Torfajökull (Soosalu et al., 2006-this issue). Such a feature may, as well, be the cause of seismicity at Skaftárkatlar area under the Vatnajökull ice cap (Björnsson and Einarsson, 1990). These two sites, together with Torfajökull, are the only sources of persistent low-frequency seismicity in Iceland. Other seismically active Icelandic volcanoes produce mostly high-frequency events.

Geodetic measurements can assist in testing the validity of the cryptodome interpretation. With the current layout of the geodetic network in the Torfajökull area (Ólafsdóttir et al., 2003) measurements cannot confirm or dismiss the presence of a cryptodome. The deformation field of a shallow cryptodome is very localised and detectable only at close distances (e.g. Soosalu et al., 2006-this issue). The closest tilt station, near the seismic station HRAF is located 7–8 km from

the area of low-frequency seismicity (Sturkell et al., 2006-this issue). At this distance, a shallow and localised source, such as the inferred cryptodome, would not give any signal (Sturkell, E., pers. comm., 2004). Interferometric combination of synthetic aperture radar (InSAR) satellite images covering the Torfajökull area has been performed. Coherence in the area of interest is however low, due to local glacial cover (Pedersen, R., pers. comm., 2004).

Our dense seismic network demonstrated that the low-frequency events are a persistent feature at Torfajökull, observed even on a daily basis. However, a major part of this seismicity is not detectable with stations further than a few kilometres away. Our network could provide quite reliable epicentral estimates for the largest of the low-frequency events. The hypocentral accuracy is not as good, because the closest stations were 7–8 km away from the locus of the activity. However, it is obvious that these events are shallow. None were observed deeper than at 14 km depth, and most likely the centre of activity is located at shallower depth.

The swarm-like behaviour of the low-frequency Torfajökull events needs further research. If the cryptodome interpretation is correct, the fluctuation of seismicity may be directly related to the state of activity of the dome-building process. Currently, Torfajökull is not considered likely to erupt in the near future, but it still is a highly active volcano, capable of producing major explosive eruptions. Further monitoring of the low-frequency seismicity of Torfajökull may give important information for its eruptive scenarios.

5. Conclusions

Low-frequency earthquakes are a persistent feature of the seismicity at the Torfajökull volcano. They cluster tightly in a small area in the southern part of the caldera and appear to be shallow. They are small in size (M_L typically ≤ 1), and often occur in swarms. The activity can vary considerably, from a few hundred events per day to practically no detectable activity. They are very monochromatic, with dominant frequencies around 1–2 Hz, have small and emergent P-phases and a later, more distinct phase, which we used as an S-arrival.

We hypothesise that the low-frequency earthquakes at Torfajökull are expressions of a shallow cryptodome in some sort of state of activity. Our interpretation is supported by the following facts: 1) seismicity is very localised, 2) the low-frequency activity coincides with the locations of highest temperature geothermal areas

within the volcano, 3) Torfajökull is a rhyolitic volcano dominated by dome-building activity.

Acknowledgements

We are grateful to Bob White and the SEIS-UK instrument pool for lending the portable seismometers, which provided the essential data set of the low-frequency events. Icelandic Meteorological Office gathered the additional digital data. The National Power Company of Iceland funds the maintenance of the analogue stations. Alex Bourne is thanked for instructing us to use the system, both in the field and in the office. We thank Andrew Myers and Paul Denton from SEIS-UK for technical and computer assistance. Halldór Ólafsson and Haukur Brynjólfsson are acknowledged for invaluable work and expertise during all phases of the fieldwork. Good and careful field assistance was also given by Antoine Dailloux, Alison Hibbs, Fredrik Holm, Matti Horttanainen, Eyjólfur Magnússon, Andy Malone, Susan Pitts, and Bob and Jim White. Steven Sherburn provided many useful suggestions and advices for data analysis. Frederik Tilmann allowed us to use his correlation code. R.L. was supported by the FWF Erwin-Schrödinger Fellowship J2264-NO7. All the figures, except Fig. 9 were made using the GMT public domain software (Wessel and Smith, 1998). Comments by two anonymous reviewers and editor Peggy Hellweg improved the manuscript.

References

- Almendros, J., Ibáñez, J.M., Alguacil, G., Del Pezzo, E., Ortiz, R., 1997. Array tracking of the volcanic tremor source at Deception Island, Antarctica. *Geophys. Res. Lett.* 24, 3069–3072.
- Arnórsson, S., Ívarsson, G., Cuff, K.E., Sæmundsson, K., 1987. Geothermal activity in the Torfajökull field South Iceland: summary of geochemical studies. *Jökull* 37, 1–12.
- Bjarnason, J.Ö., Ólafsson, M., 2000. Chemical composition of geothermal steam and hot water at Torfajökull. National Energy Authority of Iceland, Report OS-2000/030. 91 pp. (in Icelandic).
- Björnsson, H., Einarsson, P., 1990. Volcanoes beneath Vatnajökull, Iceland: evidence from radio echo-sounding, earthquakes and jökulhlaups. *Jökull* 40, 147–168.
- Böðvarsson, R., Rögnvaldsson, S.Th., Slunga, R., Kjartansson, E., 1999. The SIL data acquisition system—at present and beyond year 2000. *Phys. Earth Planet. Int.* 113, 89–101.
- Brandadóttir, B., Einarsson, P., 1992. Volcanic tremor and low-frequency earthquakes in Iceland. In: Gasparini, P., Scarpa, R., Aki, K. (Eds.), *Volcanic Seismology*. Springer, Berlin, pp. 212–222.
- Chouet, B.A., 1996. Long-period volcano seismicity: its source and use in eruption forecasting. *Nature* 380, 309–316.
- Donnadieu, F., Merle, O., Besson, J.-C., 2001. Volcanic edifice stability during cryptodome intrusion. *Bull. Volcanol.* 63, 61–72.
- Einarsson, P., 1991. Earthquakes and present-day tectonism in Iceland. *Tectonophysics* 189, 261–279.

- Einarsson, P., Sæmundsson, K., 1987. Earthquake epicenters 1982–1985 and volcanic systems in Iceland (map). In: Sigfússon, Þ.I. (Ed.), *Í hlutarins eðli*, Festschrift for Þorbjörn Sigurgeirsson. Menningarsjóður, Reykjavík.
- Grönvold, K., Óskarsson, N., Johnsen, S.J., Clausen, H.B., Hammer, C.U., Bond, G., Bard, E., 1995. Ash layers from Iceland in the Greenland GRIP ice core correlated with oceanic and land sediments. *Earth Planet. Sci. Lett.* 135, 149–155.
- Gunnarsson, B., Marsh, B.D., Taylor Jr., H.P., 1998. Generation of Icelandic rhyolites: silicic lavas from the Torfajökull central volcano. *J. Volcanol. Geotherm. Res.* 83, 1–45.
- Jakobsson, S.P., 1979. Petrology of Recent basalts of the Eastern Volcanic Zone, Iceland. *Acta Nat. Isl.* 26, 1–103.
- Jóhannesson, H., Sæmundsson, K., 1989. Geological map of Iceland. 1:500000. Bedrock geology, first edition. Icelandic Museum of Natural History and Iceland Geodetic Survey, Reykjavík.
- Jóhannesson, H., Jakobsson, S.P., Sæmundsson, K., 1990. Geological map of Iceland, sheet 6, South Iceland, third edition. Icelandic Museum of Natural History and Iceland Geodetic Survey, Reykjavík.
- Klein, F.W., 1978. Hypocenter location program HYPOINVERSE. Open-File Rep.-U.S. Geol. Surv. 78-694 (113 pp.).
- Lahr, J., 1999. Hypoellipse. A computer program for determining local earthquake hypocentral parameters, magnitude, and first-motion pattern (Y2K) compliant version). Open-file report 99-23, on-line version. United States Geological Survey.
- Larsen, G., 1984. Recent volcanic history of the Veidivötn fissure swarm, southern Iceland—an approach to volcanic risk assessment. *J. Volcanol. Geotherm. Res.* 22, 33–58.
- Lippitsch, R., White, R.S., Soosalu, H., 2005. Precise hypocentre relocation of microearthquakes in a high-temperature geothermal field: the Torfajökull central volcano, Iceland. *Geophys. J. Int.* 160, 370–387.
- Lomax, A., Curtis, A., 2001. Fast, probabilistic earthquake location in 3D models using Oct-Tree importance sampling. *Geophys. Res. Abstr.* 3.
- Lomax, A., Virieux, J., Volant, P., Thierry-Berge, C., 2000. Probabilistic earthquake location in 3D and layered models. In: Thurber, C.H., Rabinowitz, N. (Eds.), *Advances in Seismic Events Location*. Kluwer Acad., Norwell, Mass, pp. 101–134.
- McGarvie, D.W., 1984. Torfajökull: a volcano dominated by magma mixing. *Geology* 12, 685–688.
- McGarvie, D.W., 1985. Volcanology and petrology of mixed magmas and rhyolites from the Torfajökull Volcano, Iceland. PhD thesis, Univ. Lancaster, 255 pp.
- McNutt, S.R., 2000. Volcanic seismicity. In: Sigurðsson, H. (Ed.), *Encyclopedia of Volcanoes*. Academic Press, San Diego, pp. 1015–1033.
- Minakami, T., 1974. Seismology of volcanoes in Japan. In: Civetta, L., Gasparini, P., Luongo, G., Rapolla, A. (Eds.), *Physical Volcanology*. Elsevier, Amsterdam, pp. 1–27.
- Moser, T.J., van Eck, T., Nolet, G., 1992. Hypocentre determination in strongly heterogeneous earth models using the shortest path method. *J. Geophys. Res.* 97, 6563–6572.
- Okada, Hm., Watanabe, H., Yamashita, H., Yokoyama, I., 1981. Seismological significance of the 1977–1978 eruptions and the magma intrusion process of Usu volcano, Hokkaido. *J. Volcanol. Geotherm. Res.* 9, 311–334.
- Ólafsdóttir, R., Sturkell, E., Ólafsson, H., Þorbergsson, G., Einarsson, P., Rennen, M., Geirsson, H., Theódórsson, Th., 2003. GPS points in Iceland, 1986–2002. Nordic Volcanological Institute Report 0301. 411 pp. (in Icelandic).
- Óskarsson, N., Sigvaldason, G.E., Steinþórsson, S., 1982. A dynamic model of rift zone petrogenesis and the regional petrology of Iceland. *J. Petrol.* 23, 28–74.
- Riggs, N., Carrasco-Nunez, G., 2004. Evolution of a complex isolated dome system, Cerro Pizarro, central Mexico. *Bull. Volcanol.* 66, 322–335.
- Ruiz, M., Guillier, B., Chatelain, J.-L., Yepes, H., Hall, M., Ramon, P., 1998. Possible causes for the seismic activity observed in Cotopaxi volcano, Ecuador. *Geophys. Res. Lett.* 25, 2305–2308.
- Sæmundsson, K., 1972. Geological notes on the Torfajökull area. *Náttúrufræðingurinn* 42, 81–99 (in Icelandic).
- Sæmundsson, K., 1982. Calderas in the neovolcanic zones of Iceland. *Eldur er í Norðri*, Festschrift for Sigurður Þórarinnsson. Sögufélag, Reykjavík, pp. 221–239 (in Icelandic).
- Sherburn, S., Bryan, C.J., Hurst, A.W., Latter, J.H., Scott, B.J., 1999. Seismicity of Ruapehu volcano, New Zealand, 1971–1996: a review. *J. Volcanol. Geotherm. Res.* 88, 255–278.
- Simiyu, S.M., Keller, G.R., 2000. Seismic monitoring of the Olkaria geothermal area, Kenya rift valley. *J. Volcanol. Geotherm. Res.* 95, 197–208.
- Soosalu, H., Einarsson, P., 1997. Seismicity around the Hekla and Torfajökull volcanoes, Iceland, during a volcanically quiet period, 1991–1995. *Bull. Volcanol.* 59, 36–48.
- Soosalu, H., Einarsson, P., 2004. Seismic constraints on magma chambers at Hekla and Torfajökull volcanoes, Iceland. *Bull. Volcanol.* 66, 276–286.
- Soosalu, H., Jónsdóttir, K., Einarsson, P., 2006. Seismicity crisis at the Katla volcano, Iceland—signs of a cryptodome? *J. Volcanol. Geotherm. Res.* 153, 177–186 doi:10.1016/j.jvolgeores.2005.10.013.
- Stammler, K., 1992. Seismic Handler, User's Manual. Seismisches Zentralobservatorium Graefenberg, Erlangen. 32 pp.
- Stefánsson, R., Böðvarsson, R., Slunga, R., Einarsson, P., Jakobsdóttir, S., Bungum, H., Gregersen, S., Havskov, J., Hjelme, J., Korhonen, H., 1993. Earthquake prediction research in the South Iceland Seismic Zone and the SIL project. *Bull. Seismol. Soc. Am.* 83, 696–716.
- Sturkell, E., Einarsson, P., Sigmundsson, F., Geirsson, H., Ólafsson, H., Pedersen, R., de Zeeuw-van Dalen, E., Linde, A.L., Sacks, I.S., Stefánsson, R., 2006. Volcano geodesy and magma dynamics in Iceland. *J. Volcanol. Geotherm. Res.* doi:10.1016/j.jvolgeores.2005.07.010.
- Tarantola, A., Valette, B., 1982. Inverse problems = quest for information. *J. Geophys. Res.* 50, 159–170.
- Waldhauser, F., Ellsworth, W.L., 2000. A double-difference earthquake location algorithm: method and application to the northern Hayward fault, California. *Bull. Seismol. Soc. Am.* 90, 1353–1368.
- Waldhauser, F., Ellsworth, W.L., 2002. Fault structure and mechanics of the Hayward fault, California, from double-difference earthquake locations. *J. Geophys. Res.* 107, B3:2054. doi:10.1029/2001JB000084.
- Weaver, C.S., Malone, S.D., 1976. Mt. Saint Helens seismic events: volcanic earthquakes or glacial noises? *Geophys. Res. Lett.* 3, 197–200.
- Wessel, P., Smith, W.H.F., 1998. New, improved version of the Generic Mapping Tools released. *Eos* 79, 579.
- Wolfe, C., Bjamason, I.Þ., VanDecar, J.C., Solomon, S.C., 1997. Seismic structure of the Iceland mantle plume. *Nature* 385, 245–247.